Hindawi
Shock and Vibration
Volume 2019, Article ID 5308209, 12 pages
https://doi.org/10.1155/2019/5308209

Research Article

Dynamic Responses of Vehicle-CRTS III Slab Track System and Vehicle Running Safety Subjected to Uniform Seismic Excitation

Ping Lou,[1,2] **Kailun Gong**,[1,2,3] **Chen Zhao**,[1,2] **Qingyuan Xu**,[1] **and Robert K. Luo**[1,4]

[1]*School of Civil Engineering, Central South University, Changsha, China*
[2]*Key Laboratory of Heavy Railway Engineering Structure of Education Ministry, Changsha 410075, China*
[3]*China Railway Engineering Consulting Group Co., Ltd., Beijing, China*
[4]*Department of Engineering and Technology, Trelleborg IAVS, Leicester, UK*

Correspondence should be addressed to Qingyuan Xu; xuqingyuan1972@163.com

Received 17 April 2019; Revised 17 June 2019; Accepted 2 July 2019; Published 21 July 2019

Academic Editor: Franck Poisson

The dynamic model for the vehicle-CRTS III slab track system is established subjected to uniform seismic excitation, and the calculation program with MATLAB is compiled and verified. The influences of track parameters, seismic intensity, and running speed of the vehicle on the dynamic responses of the system and the vehicle running safety are analyzed. The results show that (1) the track parameters have certain influence on the dynamic responses of the system, and the seismic intensity and the running speed of the vehicle have important influence on the vehicle running safety; (2) the derailment coefficient is highly sensitive to seismic intensity, and the wheel load reduction rate is also highly sensitive to the running speed of the vehicle.

1. Introduction

Many scholars have studied the dynamic responses of the vehicle-bridge (track) system subjected to seismic excitation. Tanabe et al. [1] developed a new method for calculating the dynamic response of track results under seismic excitation. Nishimura et al. [2] specifically studied the impact of structural strength changes under rails on vehicle running safety under seismic excitation. Ling et al. [3] investigated the effects of seismic wave spectral characteristics on derailment of high-speed railway vehicles under earthquake excitation. Xiang et al. [4] transformed the structure into the ESDF system and analyzed the dynamic characteristics of the structure to vertical seismic excitation. Mylona et al. [5] investigated the dynamic response of piers on pile foundations under combined translational and rotational seismic excitation. Li et al. [6] used SVGM as input of seismic analysis and analyzed its dynamic response of long-span frame bridges. Deshan et al. [7] studied the vulnerability of bridges to major and after-shock excitations. Guo et al. [8] independently developed the joint simulation program and analyzed the safety of bridge driving under the influence of earthquake. Du et al. [9] analyzed the dynamic response of the vehicle-bridge system with nonuniform seismic excitation based on the finite element method. Zhang et al. [10] calculated the dynamic response of a vehicle-bridge system under multisupported seismic excitation. Chen [11] studied dynamic responses of the high-speed railway simply supported girder bridge and CRTS II slab track under earthquake action. Shaban et al. [12] evaluated the effects of vehicles on the seismic response of bridges by applying five different seismic excitation tests. Paraskeva et al. [13] researched the dynamic response of a vehicle-bridge interacting system under vertical earthquake excitation.

The CRTS III slab track is a new type of track structure with independent intellectual property right in China. The main difference between CRTS III slab track and the other two types of slab track, i.e., CRTS I slab track, CRTS II slab track lies in the use of self-compacting concrete between slab and base rather than cement asphalt mortar. The main mechanical characteristic of CRTS III slab track is that the

self-compacting concrete is bonded with the slab to form a composite slab structure, which bears the train load together. The CRTS III slab track has been widely used in passenger dedicated railways and most of the passenger dedicated railway lines cross the seismic zone [14]. Once an earthquake occurs, it will cause immeasurable damage to track structures. However, less research has been done on the dynamic responses of the vehicle-CRTS III slab track system subjected to seismic excitation. Therefore, it is urgent to study the influences of CRTS III slab track parameters, seismic intensity, and running speed of the vehicle on the dynamic responses of the system across seismic fault zone and to reduce the damage of track and ensure the vehicle running safety.

2. Dynamic Model for Vehicle-CRTS III Slab Track System during Seismic Excitation

2.1. Vehicle Model. The vehicle is modeled as a mass-spring-damper system consisting of a car body, two bogie frames, four wheelsets, and two-stage suspensions. The car body, each bogie frame, and each wheelset are modeled as a rigid body, respectively. The primary suspension between each wheelset and each bogie frame and the secondary suspension between car body and each bogie frame are modeled as spring and shock absorber. The longitudinal motion of the vehicle is not considered. The number of degrees of freedom for car body and each bogie frame is 5. The vertical displacement and roll rotation for each wheelset depend on the vertical displacement of rails; the independent degrees of freedom for each wheelset become 2. Consequently, the total number of independent degrees of freedom for the vehicle is 23.

2.2. Model for CRTS III Slab Track. The CRTS III slab track from top to bottom consists of rail, fastener, slab, self-compacting concrete layer, isolation layer (in this paper, it is replaced by cushion layer), and base. The longitudinal motion of track is also not considered. The rail is modeled as a finite length linear elastic Euler beam, and the fastener is modeled as a spring and shock absorber. The slab and self-compacting concrete layer are equivalent to composite slab, and the composite slab and the base are modeled as many slab elements. The cushion layer and the subgrade below the base are modeled as springs and damping absorbers. The neutral plane location for the composite slab is determined by the following equation [15]:

$$h_0 = \frac{E_1 h_1^2 + 2E_2 h_1 h_2 + E_2 h_2^2}{2\left(E_1 h_1 + E_2 h_2\right)}, \tag{1}$$

where h_0 is the height from the neutral plane location to the top of the composite slab, E_1 and E_2 are the elastic modulus of the slab and self-compacting concrete layer, respectively, and h_1 and h_2 are the thickness of the slab and self-compacting concrete layer, respectively.

The bending stiffness and the equivalent modulus of elasticity of composite slab can be written as [15]

$$\begin{aligned} D_0 &= \frac{E_1}{3}\left[h_0^3 - (h_0 - h_1)^3\right] \\ &\quad + \frac{E_2}{3}\left[(h_0 - h_1)^3 + (h_1 + h_2 - h_0)^3\right], \\ E_0 &= \frac{D_0}{I}, \end{aligned} \tag{2}$$

where D_0 and E_0 are the bending stiffness and the equivalent modulus of elasticity of composite slab, respectively, and I is the moment of inertia of composite slab.

The dynamic model for the vehicle-CRTS III slab track system is shown in Figure 1, and the track parameters shown in Table 1 are taken from the measured data of the Chengguan Railway mentioned in the literature [16].

2.3. Equation of Motion for the Vehicle-CRTS III Slab Track System. The vibration equation of motion for the vehicle-CRTS III slab track system subjected to seismic excitation can be written as

$$\begin{aligned} &\begin{bmatrix} \mathbf{M}_{\mathrm{v}} & & & \\ & \mathbf{M}_{\mathrm{rr}} & & \\ & & \mathbf{M}_{\mathrm{ss}} & \\ & & & \mathbf{M}_{\mathrm{dd}} \end{bmatrix} \begin{Bmatrix} \ddot{\mathbf{Z}}_{\mathrm{v}} \\ \ddot{\mathbf{Z}}_{\mathrm{r}} \\ \ddot{\mathbf{Z}}_{\mathrm{s}} \\ \ddot{\mathbf{Z}}_{\mathrm{d}} \end{Bmatrix} \\ &+ \begin{bmatrix} \mathbf{C}_{\mathrm{v}} & \mathbf{C}_{\mathrm{v-r}} & & \\ \mathbf{C}_{\mathrm{r-v}} & \mathbf{C}_{\mathrm{rr}} & \mathbf{C}_{\mathrm{r-s}} & \\ & \mathbf{C}_{\mathrm{s-r}} & \mathbf{C}_{\mathrm{ss}} & \mathbf{C}_{\mathrm{s-d}} \\ & & \mathbf{C}_{\mathrm{d-s}} & \mathbf{C}_{\mathrm{dd}} \end{bmatrix} \begin{Bmatrix} \dot{\mathbf{Z}}_{\mathrm{v}} \\ \dot{\mathbf{Z}}_{\mathrm{r}} \\ \dot{\mathbf{Z}}_{\mathrm{s}} \\ \dot{\mathbf{Z}}_{\mathrm{d}} \end{Bmatrix} \\ &+ \begin{bmatrix} \mathbf{K}_{\mathrm{v}} & \mathbf{K}_{\mathrm{v-r}} & & \\ \mathbf{K}_{\mathrm{r-v}} & \mathbf{K}_{\mathrm{rr}} & \mathbf{K}_{\mathrm{r-s}} & \\ & \mathbf{K}_{\mathrm{s-r}} & \mathbf{K}_{\mathrm{ss}} & \mathbf{K}_{\mathrm{s-d}} \\ & & \mathbf{K}_{\mathrm{d-s}} & \mathbf{K}_{\mathrm{dd}} \end{bmatrix} \begin{Bmatrix} \mathbf{Z}_{\mathrm{v}} \\ \mathbf{Z}_{\mathrm{r}} \\ \mathbf{Z}_{\mathrm{s}} \\ \mathbf{Z}_{\mathrm{d}} \end{Bmatrix} = \begin{Bmatrix} \mathbf{F}_{\mathrm{v}} \\ \mathbf{F}_{\mathrm{r}} \\ \mathbf{F}_{\mathrm{s}} \\ \mathbf{F}_{\mathrm{d}} \end{Bmatrix}, \end{aligned} \tag{3}$$

where **M**, **C,** and **K** denote the mass, damping, and stiffness matrices, respectively, **F** denotes the force vector, and the subscripts v, r, s, and d denote the vehicle, rail, composite slab, and base, respectively. In order to reduce the length of the article, the detailed expression of the equation is omitted. In the force vector, two different excitations are considered. One is the track irregularity, and the other is earthquake. China high-speed track spectrum is adopted for track irregularity. Imperial Valley-02 and San Fernando seismic records from the strong ground motion database of the western United States are used. According to the Code for Seismic Design of Railway Engineering [17], the seismic intensity of ground motion is adjusted to 0.1 g and is loaded at the lower boundary of the system with the ratio 1 : 0.65 of the lateral acceleration to vertical acceleration.

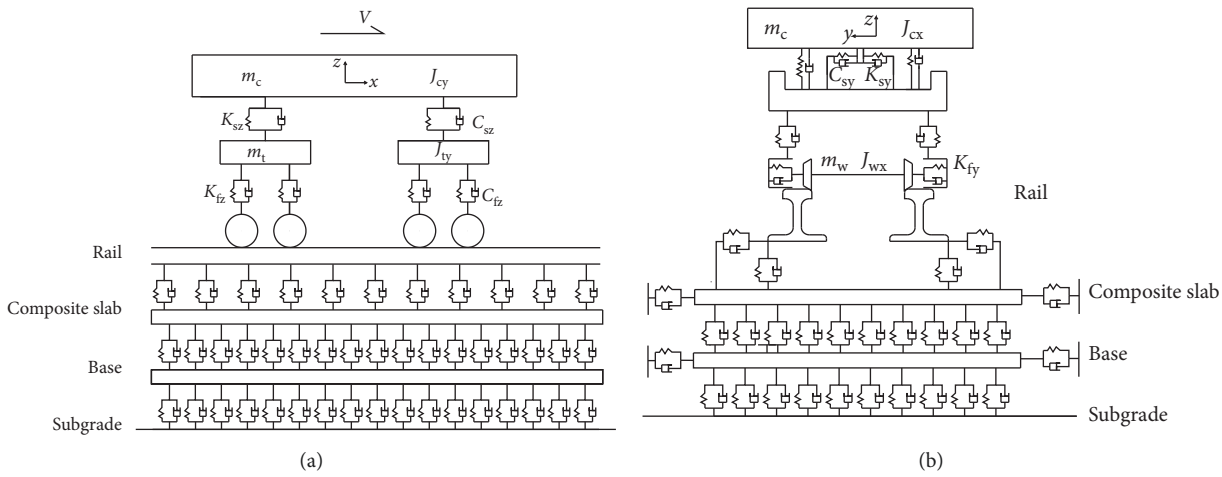

Figure 1: The dynamic model for the vehicle-CRTS III slab track system. (a) Face view. (b) Side view.

Table 1: The parameters of track.

Notation	Item	Value
m_r	Unit length mass of rail	60.64 kg/m
E_r	Elastic modulus of rail	2.059×10^{11} N/m^2
I_r	Moment of inertia of rail	3.217×10^{-5} m^4
L_{rs}	Space of fastener	0.65 m
K_{rsz}	Vertical stiffness of fastener	2.5×10^7 N/m
C_{rsz}	Vertical damping of fastener	2.6×10^4 N·s/m
K_{rsy}	Lateral stiffness of fastener	5×10^7 N/m
C_{rsy}	Lateral damping of fastener	1.24×10^4 N·s/m
E_s	Elastic modulus of slab	3.65×10^{10} N/m^2
ρ_s	Density of slab	2500 kg/m^3
E_c	Strength of self-compacting concrete layer	3.25×10^{10} N/m^2
K_{sdz}	Surface stiffness of cushion layer	400 MPa/m
C_{sdz}	Surface damping of cushion layer	3.43×10^4 Pa·s/m
E_b	Elastic modulus of base	3.25×10^{10} N/m^2
ρ_b	Density of base	2500 kg/m^3

Equation (3) can be solved by the step-by-step integration method, such as Newmark-β method [18] or Wilson-θ method [19], to obtain the dynamic responses of the vehicle and track.

3. Model Verification

The vehicle runs on the track at 250 km/h. For the excitation source, only the track irregularity is considered. The time history curve of calculated wheel-rail vertical force and base vertical acceleration is shown in Figure 2, and the maximum values of calculated and measured dynamic responses of the vehicle-track system are presented in Table 2. Table 2 shows that the calculated maximum values are basically the same as the measured ones. Therefore, it is helpful to illustrate the correctness of the proposed model.

4. Influence of Track Parameters on the Dynamic Response of the Vehicle-Track System under Seismic Excitation

In this section, the seismic intensity with 0.1 g of ground motion for Imperial Valley-02 seismic records, the running speed of 300 km/h, and the normal track parameters shown in Table 1 are adopted. In Sections 4.1–4.3, only the single parameter is changed, and the other parameters are the same as the normal case.

4.1. Influence of Fastener Stiffness. The fastener stiffness plays a significant part in vibration reduction and energy transfer of track. In order to analyze the influence of fastener stiffness on the dynamic responses of the vehicle-track system under seismic excitation, the values of 2.5×10^7 N/m, 4.0×10^7 N/m, 5.0×10^7 N/m, 6.0×10^7 N/m, and 7.0×10^7 N/m are adopted. The maxima of the dynamic responses of the vehicle-track system with different fastener stiffnesses are plotted in Figure 3.

As shown in Figure 3(a), the maxima of the vertical accelerations of composite slab and base increase with the increase of fastener stiffness, and the increment of base is smaller than that of the composite slab. When the stiffness is between 2.5×10^7 N/m and 4.0×10^7 N/m, the acceleration increases fastest, and the stiffness is between 4.0×10^7 N/m and 7.0×10^7 N/m, the acceleration increases gradually slowed. It can be found in Figure 3(b) that the maxima of the wheel-rail vertical and lateral forces increase with the increase of fastener stiffness; however, the increment is small. The explanations are as follows. With the increase of the stiffness of fastener, the restraint between rail and composite slab increases, then the wheel-rail force increases, and the length range of rail bearing wheel load decreases. Therefore, the load acting on composite slab increases, which leads to the increase of the acceleration value of composite slab and base. From Figure 3(c), one can observe that the maxima of the tensile stress of composite slab in the lateral and longitudinal directions increase with the increase of fastener stiffness; however, the increment is small. The tensile stress

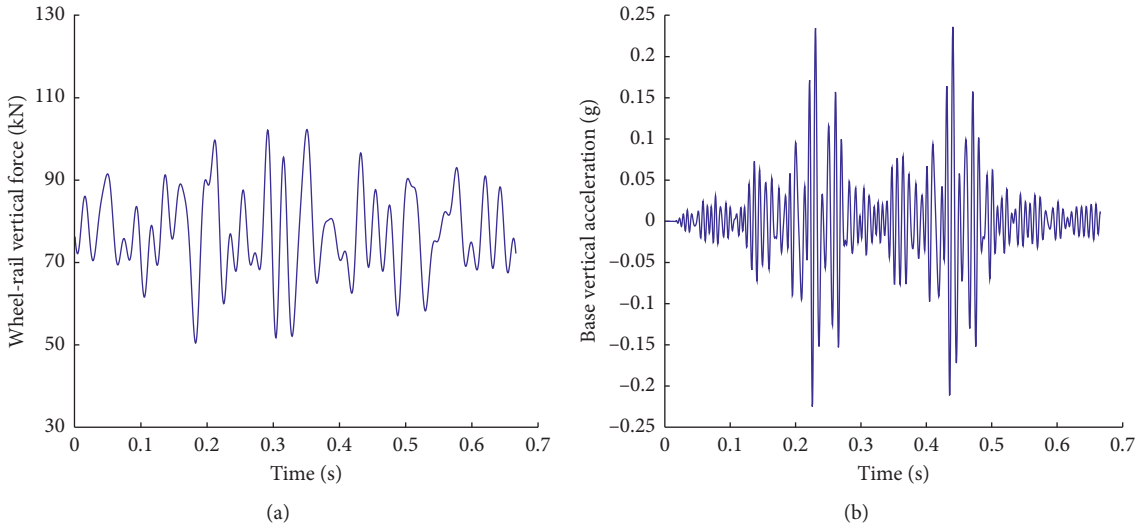

Figure 2: The time history curve of wheel-rail vertical force and base vertical acceleration. (a) Wheel-rail vertical force. (b) Base vertical acceleration.

Table 2: The maximum values of calculated and measured dynamic responses.

Dynamic responses	Wheel-rail vertical force (kN)	Rail vertical displacement (mm)	Slab vertical displacement (mm)	Base vertical acceleration (g)
Calculation	102.5	0.80	0.08	0.23
Measurement [20]	92.5	0.84	0.10	0.2

of base remains basically unchanged. Figure 3(d) shows that the change is not obvious for the maxima of the vertical displacements of rail, composite slab, and base. This is because although the stiffness of fasteners increases, the vertical wheel-rail force also increases. The vertical displacement of base is larger than that of rail because of the seismic excitation.

In general, the stiffness of fastener has influence on vertical accelerations of composite slab and base and the tensile stress of composite slab in the lateral and longitudinal directions but has little influence on the other dynamic responses of the vehicle-track system. Therefore, according to the influence law in the figures, it is suggested that the smaller stiffness of fasteners adopted is beneficial to the CRTS III slab track under earthquake.

4.2. Influence of the Modulus of Elasticity of Base. The base is the most direct structure of the system under seismic action; in order to analyze the influence of modulus of elasticity of base on the dynamic responses of the vehicle-track system under seismic excitation, the values of $1.5\times10^{10}\,\mathrm{N/m^2}$, $2.2\times10^{10}\,\mathrm{N/m^2}$, $3.25\times10^{10}\,\mathrm{N/m^2}$, and $4.0\times10^{10}\,\mathrm{N/m^2}$ are used. The maxima of the dynamic responses of the system with different moduli of elasticity of base are plotted in Figure 4.

As shown in Figure 4(a), the maxima of the vertical acceleration of base decrease with the increase of the modulus of elasticity of base, but the decrement is small, and the change of the maxima of the vertical acceleration of composite slab is not obvious. It can be found in Figure 4(b) that the influence of the modulus of elasticity of base on the wheel-rail force is also not obvious. From Figure 4(c), one can observe that the maxima of the tensile stress of composite slab and base in the lateral and longitudinal directions increase with the increase of the modulus of elasticity of base. The increases of the maxima of the tensile stress in the lateral and longitudinal directions of composite slab are 31.8% and 22.4%, respectively, and those of base are 59% and 133%, respectively. It is obvious that the tensile stress of the base is more sensitive to the change of its elastic modulus. And Figure 4(d) shows that the maxima of the vertical displacement of base decrease with the increase of its elastic modulus, but the change of the rail and composite slab is very small. The explanations are as follows. The increase of the elastic modulus of base strengthens its ability to resist deformation and thus reduces its displacement and increases its stress.

In general, the modulus of elasticity of base has important influence on the tensile stresses in the lateral and longitudinal directions of composite slab and base. However, it has little influence on the other dynamic responses of the vehicle-track system.

4.3. Influence of the Surface Stiffness of Cushion Layer. The surface stiffness of cushion layer plays a significant part in vibration reduction and energy transfer of track. The values of 200 MPa/m, 400 MPa/m, 600 MPa/m, and 1000 MPa/m are adopted to analyze the influence of surface

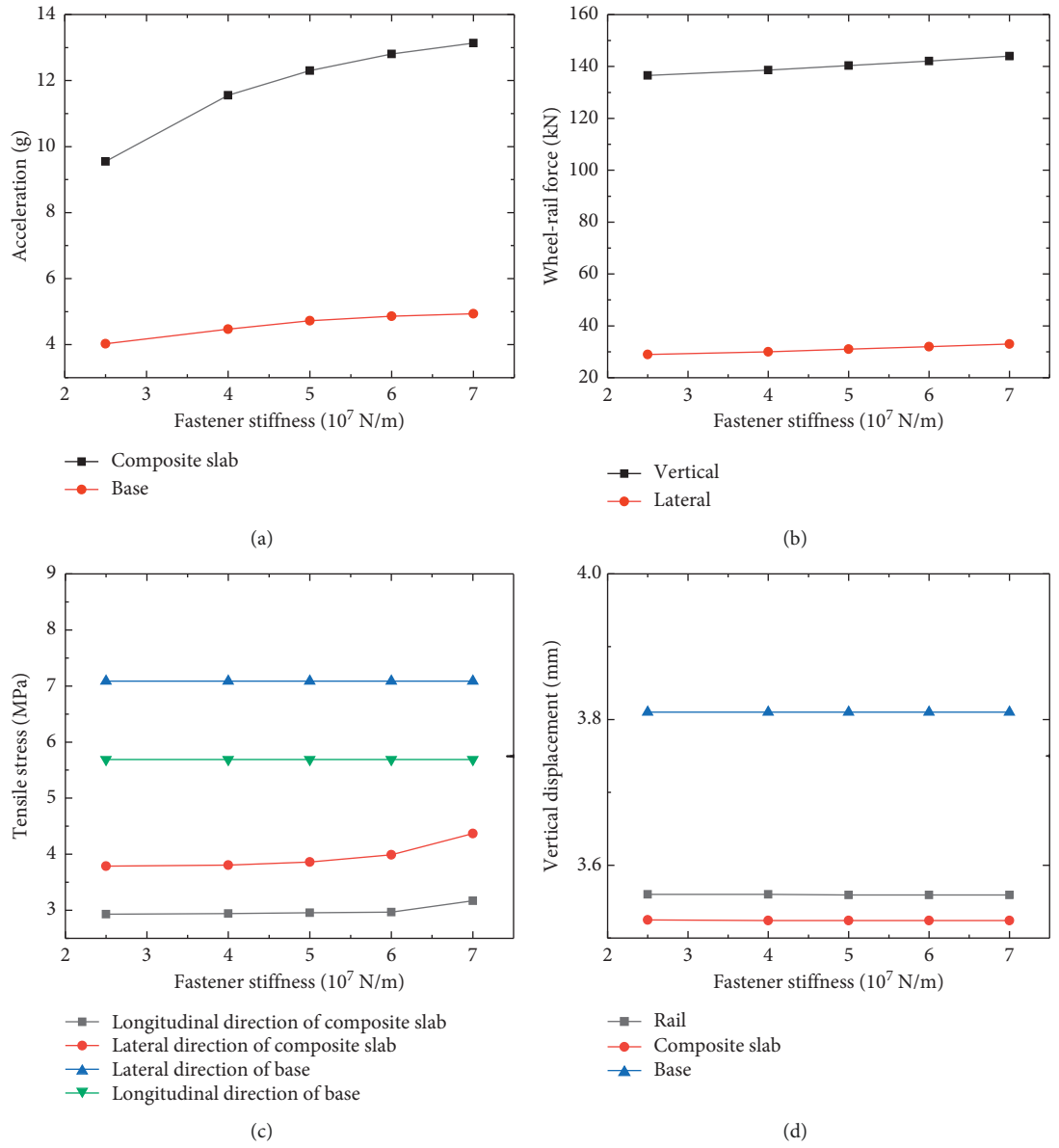

Figure 3: The maxima of the dynamic responses of the vehicle-track system with different fastener stiffnesses. (a) The vertical accelerations of composite slab and base. (b) The wheel-rail force. (c) The tensile stress of composite slab and base. (d) The vertical displacement of rail, composite slab, and base.

stiffness of cushion layer on the dynamic responses of the vehicle-track system under seismic excitation. The maxima of the dynamic responses of the vehicle-track system with different surface stiffness of cushion layer are shown in Figure 5.

As shown in Figure 5(a), with the increase of the surface stiffness of cushion layer, the maxima of the vertical acceleration of composite slab decrease; however, the maxima of the vertical acceleration of base increase. The explanations are that the vertical accelerations of composite plate and base are caused by wheel-rail force and earthquake action, and wheel-rail force is the main force. With the increase of the surface stiffness of cushion layer, the restraint between composite slab and base increases. For the composite slab, its acceleration caused by the wheel-rail force will reduce, and its acceleration caused by the earthquake action will increase; the decrement of the former is larger than the increment of the latter. Therefore, the acceleration of composite slab will reduce. For the base, its acceleration caused by the wheel-rail force will increase, and its acceleration caused by the earthquake action will reduce; the increment of the former is larger than decrement of the latter. Therefore, the acceleration of base will increase. Both of them change fastest in the range of 400–600 MPa/m. It can be found in Figure 5(b) that the influence of the surface stiffness of cushion layer on the wheel-rail force is not obvious. From Figure 5(c), one can observe that the influences of the surface stiffness of cushion layer on the maxima of the tensile stress of base in the lateral and longitudinal directions are not obvious. But the maxima of the tensile

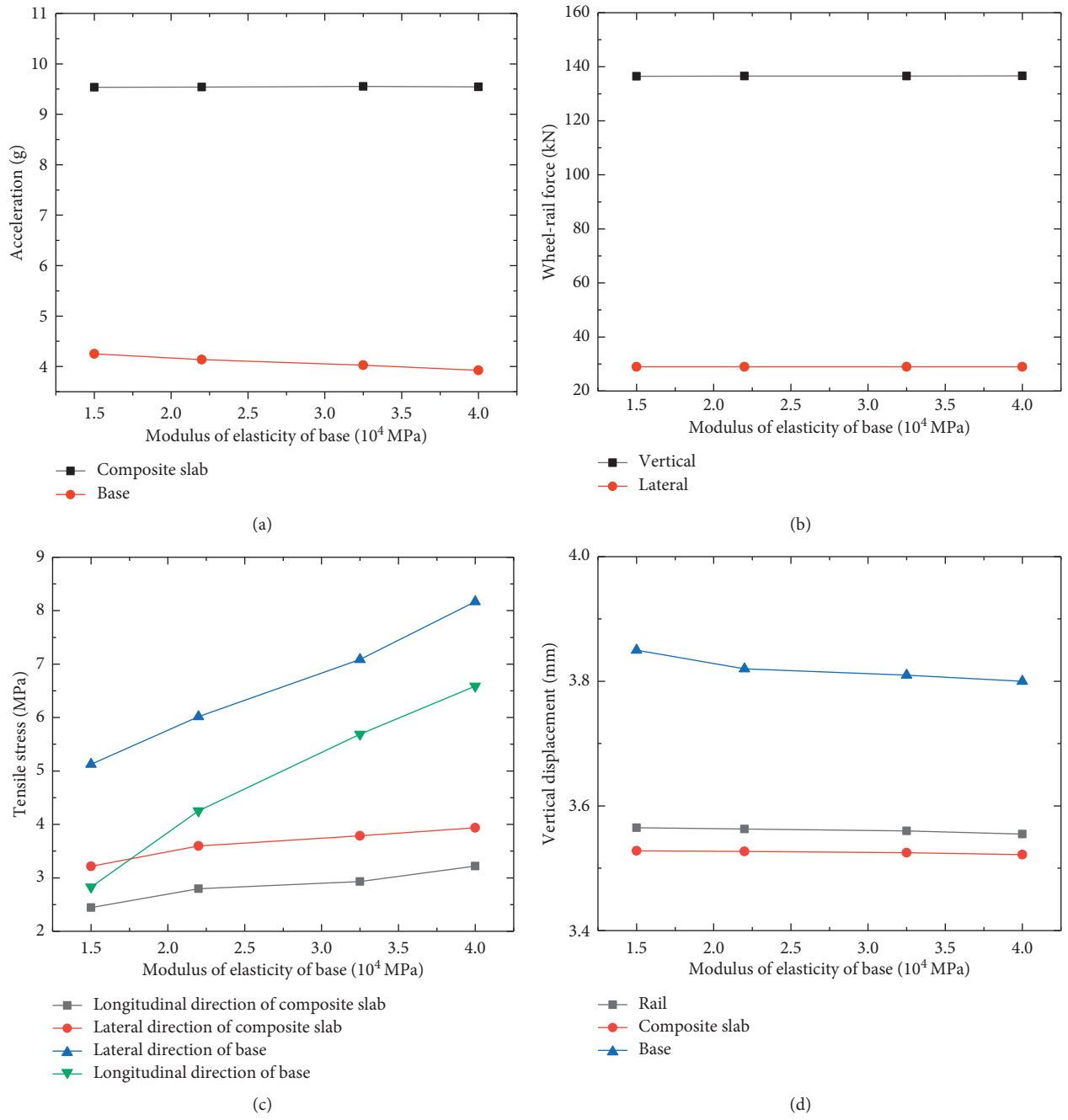

Figure 4: The maxima of the dynamic responses of the system with different moduli of elasticity of base. (a) The vertical accelerations of composite slab and base. (b) The wheel-rail force. (c) The tensile stress of composite slab and base. (d) The vertical displacement of rail, composite slab, and base.

stress of composite slab in the lateral and longitudinal directions increase with the increase of the surface stiffness of cushion layer, and they increase the fastest in the range of 400–600 MPa/m. And Figure 5(d) shows that the maxima of the vertical displacement of rail, composite slab, and base decrease with the increase of the surface stiffness of cushion layer, but their change is small.

In general, the surface stiffness of cushion layer has important influence on the vertical accelerations of composite slab and base and tensile stresses in the lateral and longitudinal directions of composite slab. However, it has little influence on the other dynamic responses of the vehicle-track system.

5. Influence of Seismic Intensity and Speed on Vehicle Running Safety

5.1. Influence of Seismic Intensity on Vehicle Running Safety. One of the aims of the vehicle-CRTS III slab track system under earthquake is to research the vehicle running safety.

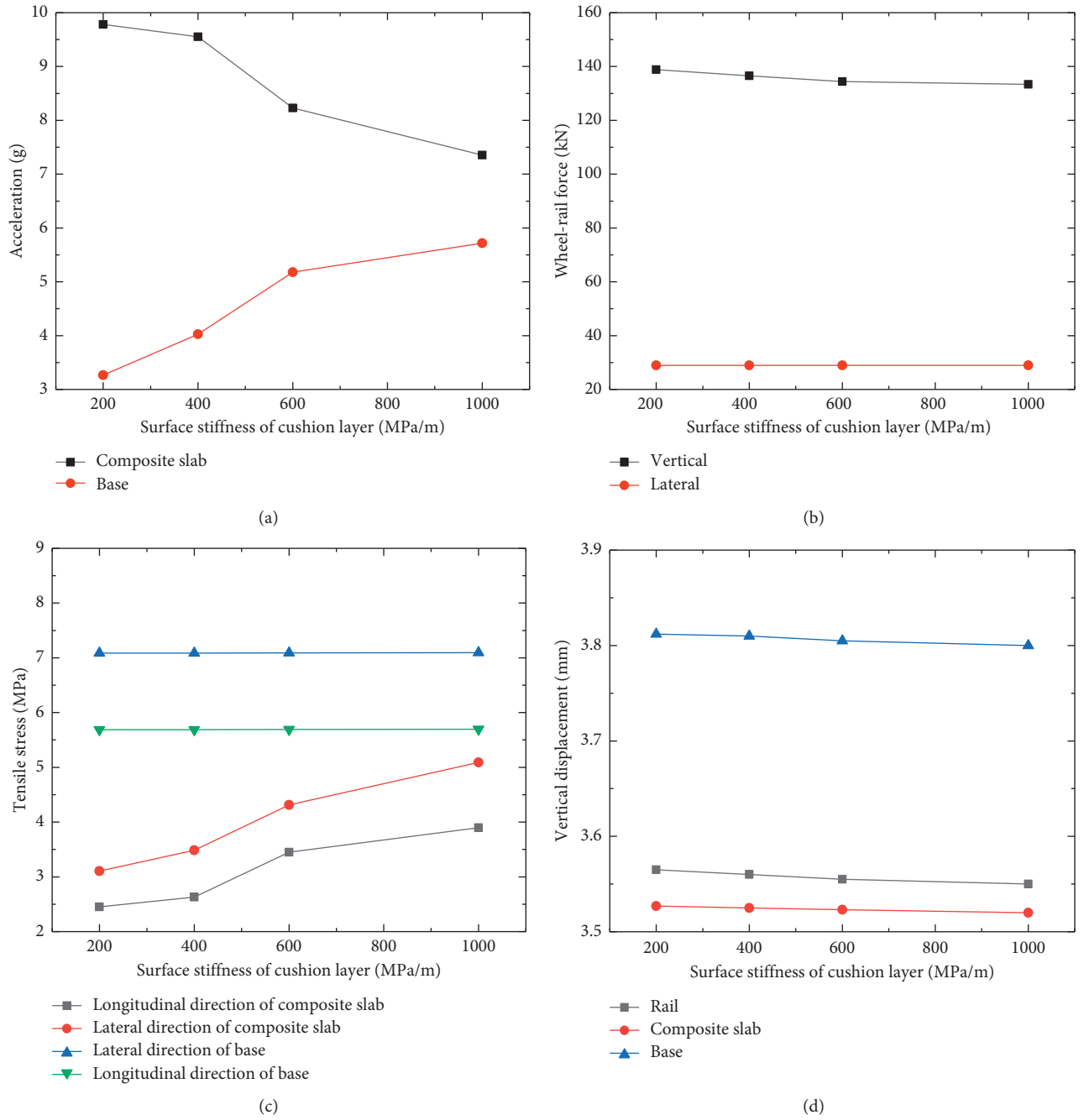

Figure 5: The maxima of the dynamic responses of the vehicle-track system with different surface stiffnesses of cushion layer. (a) The vertical accelerations of composite slab and base. (b) The wheel-rail force. (c) The tensile stress of composite slab and base. (d) The vertical displacement of rail, composite slab, and base.

Three indices of derailment coefficient, wheel load reduction rate, and wheel-rail lateral force are used to assess the operational safety of the vehicle, and their limit values [21] are listed in Table 3.

Imperial Valley-02 and San Fernando ground motion records of the same site type are used for seismic excitation, and the intensity of ground motion is 0.05 g, 0.1 g, 0.15 g, 0.2 g, 0.25 g, and 0.3 g, respectively. They are normalized by the rate of lateral to vertical accelerations with 1 : 0.65. The parameters of the vehicle and track remain unchanged, and the vehicle runs at 300 km/h. The time history curve of vertical and lateral accelerations of vehicle body under different seismic intensities is plotted in Figure 6, respectively, and the maxima of wheel-rail lateral force, wheel load reduction rate, and derailment coefficient are shown in Figure 7.

It can be found in Figure 6 that with the increase of seismic intensity, the shape of acceleration curve does not

Table 3: Limit values of running safety index.

Evaluation index of vehicle safety	Wheel-rail lateral force lateral force (kN)	Derailment coefficient	Wheel load reduction rate
Limit values	80 kN	0.8	0.6

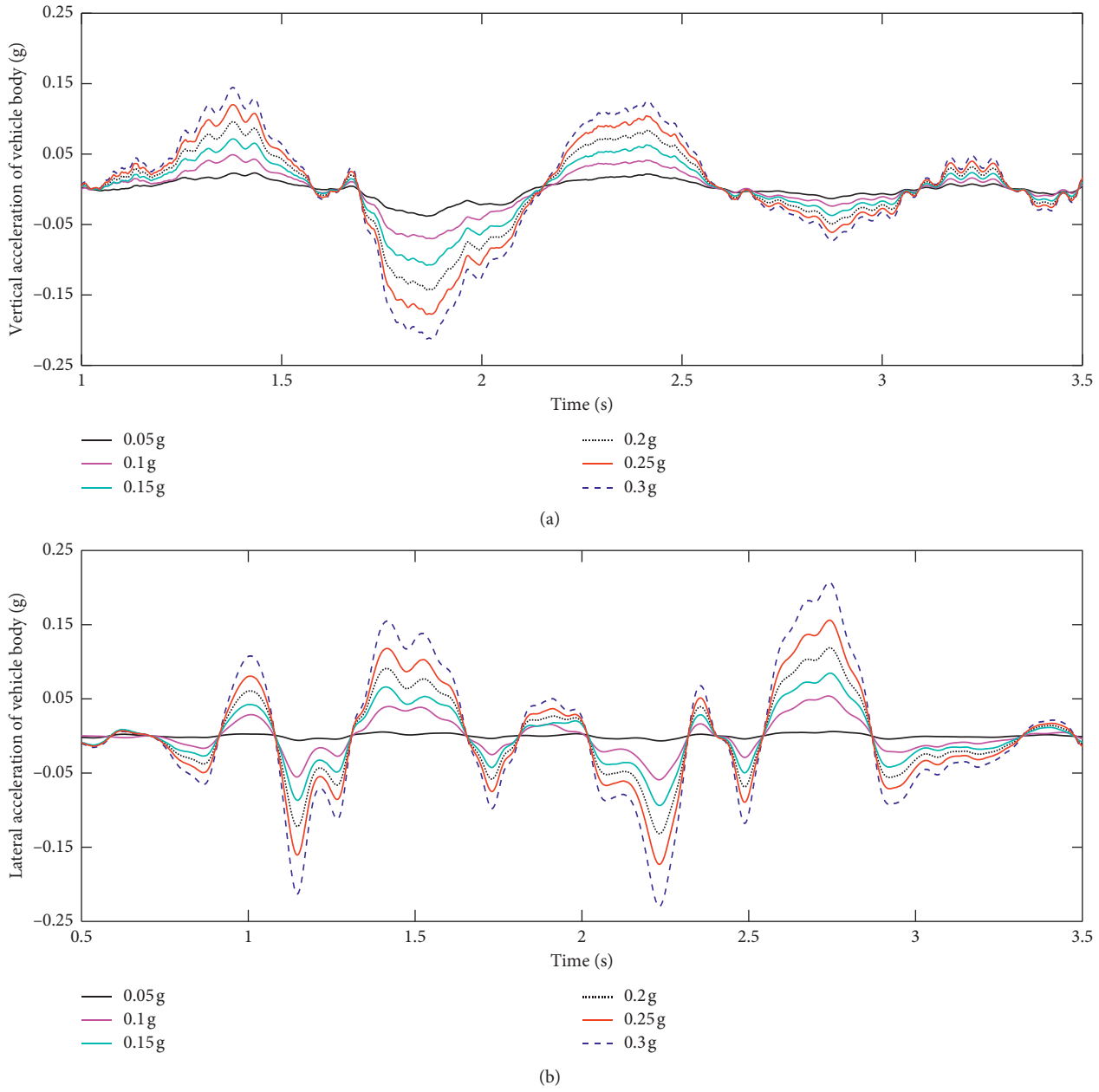

Figure 6: The time history curve of vertical and lateral accelerations of vehicle body under different seismic intensities. (a) Vertical acceleration of vehicle body. (b) Lateral acceleration of vehicle body.

change, but the peak value of each curve increases. And seismic intensity has a greater effect on lateral acceleration than vertical acceleration.

Figure 7(a) shows that the maximum of lateral force of wheel and rail increases with the increase of seismic intensity under the Imperial Valley-02 and San Fernando seismic waves. When the seismic intensity for Imperial Valley-02 wave is between 0.25 g and 0.3 g, the increment of the maximum of lateral force of wheel and rail increases sharply, reaching 42%. For the San Fernando wave with the intensity of 0.15 g–0.2 g, the increment is the largest. From Figure 7(b), one can observe that the maximum of wheel load reduction rate increases with the increase of seismic intensity under two seismic waves. For the action of Imperial Valley-02 wave, it increases approximately linearly and exceeds the limit value when the intensity is 0.3 g, but for the

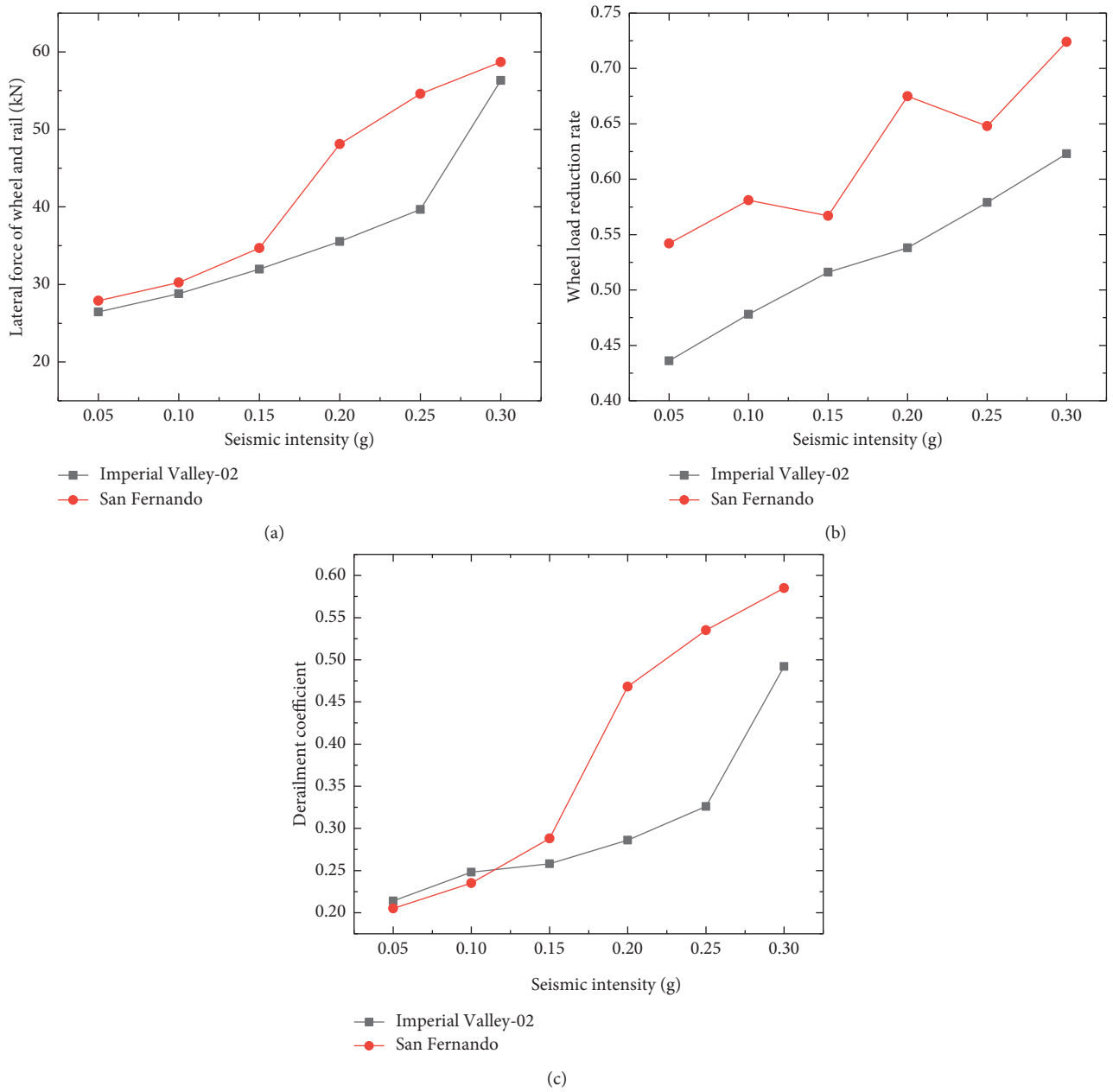

Figure 7: The maxima of wheel-rail lateral force, wheel load reduction rate, and derailment coefficient under different seismic intensities. (a) Lateral force of wheel and rail. (b) Wheel load reduction rate. (c) Derailment coefficient.

action of San Fernando wave, it fluctuates between 0.1 g and 0.25 g and exceeds the limit value when the intensity is 0.2 g. Figure 7(c) shows that the maximum of derailment coefficient increases with the increase of seismic intensity under two seismic waves. Before 0.1 g, the maximum of derailment coefficient under Imperial Valley-02 is larger than that of San Fernando wave, but after 0.15 g, it is larger under the San Fernando wave.

In general, the increase of seismic intensity has an influence on vehicle running safety of the vehicle, and the effect of San Fernando wave is greater. With the increase of seismic intensity, derailment coefficient increases the most, followed by wheel load reduction rate, and the maximum of wheel load reduction rate exceeds the limit value; then, it seriously affects the vehicle running safety.

5.2. Influence of Speed on Vehicle Running Safety. The speed values of 200 km/h, 225 km/h, 250 km/h, 275 km/h, 300 km/h, 325 km/h, and 350 km/h are used to investigate the influence of the speed on vehicle running safety. The intensity with 0.1 g for Imperial Valley-02 and San Fernando seismic waves is adopted. The parameters of the vehicle and track remain unchanged. The maxima of wheel-rail lateral force, wheel load reduction rate, and derailment coefficient are plotted in Figure 8.

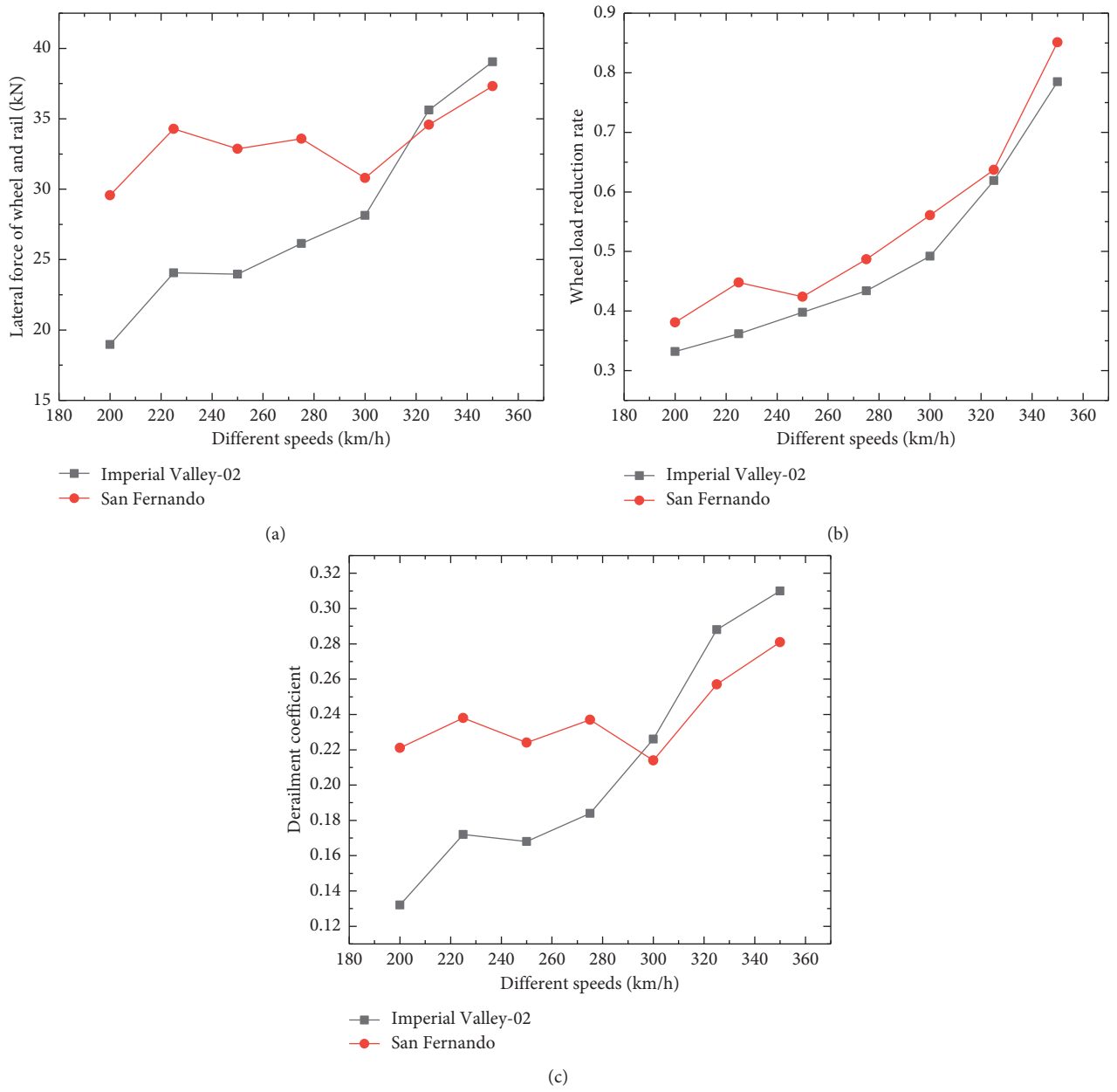

Figure 8: The maxima of wheel-rail lateral force, wheel load reduction rate, and derailment coefficient under different speeds. (a) Lateral force of wheel and rail. (b) Wheel load reduction rate. (c) Derailment coefficient.

As shown in Figure 8(a), for the action of San Fernando wave, the maximum of lateral force of wheel and rail fluctuates with the speeds between 200 km/h and 300 km/h, and it increases sharply after the speed of 300 km/h. But for the action of Imperial Valley-02 wave, the maximum of lateral force of wheel and rail increases approximately linearly with the increase of speed. Figure 8(b) shows that the maximum of wheel load reduction rate increases significantly with the increase of speed, and both of them exceed the limit value after the speed of 300 km/h. Figure 8(c) shows that the maximum of derailment coefficient increases nearly with the increase of speed under two seismic waves. The increment of the maximum of derailment coefficient under the action of San Fernando wave is smaller than that of Imperial Valley-02 wave. After the speed of 300 km/h, the maximum of derailment coefficients increase obviously under the action of two seismic waves.

In general, the maximum of wheel load reduction rate is most affected by the speed, and it exceeds the limit value after the speed of 300 km/h. Therefore, the higher the speed is, the greater the hidden danger to vehicle running safety is.

6. Conclusions

The dynamic model for the vehicle-CRTS III slab track system is established subjected to uniform seismic excitation, and the calculation program of MATLAB is compiled and verified. The influences of track parameters, seismic

intensity, and running speed of the vehicle on the dynamic responses of the system and the vehicle running safety are analyzed. The results are as follows:

(1) The stiffness of fastener has influence on vertical accelerations of composite slab and base and the tensile stress of composite slab in the lateral and longitudinal directions but has little influence on the other dynamic responses of the vehicle-track system.

(2) The modulus of elasticity of base has important influence on the tensile stresses in the lateral and longitudinal directions of composite slab and base. However, it has little influence on the other dynamic responses of the vehicle-track system.

(3) The surface stiffness of cushion layer has important influence on the vertical accelerations of composite slab and base and tensile stresses in the lateral and longitudinal directions of composite slab. However, it has little influence on the other dynamic responses of the vehicle-track system.

(4) With the increases of seismic intensity and running speed of the vehicle, the safety indices increase greatly. The derailment coefficient is highly sensitive to seismic intensity, and the running speed of the vehicle has a great influence on wheel load reduction rate. Especially, the wheel load reduction rate may exceed its limit value, which seriously affects the vehicle running safety.

Data Availability

The data used to support the findings of this study are available from the corresponding author upon request.

Conflicts of Interest

The authors declare that they have no conflicts of interest.

Acknowledgments

This work was supported by the National Key Research and Development Program of China (grant no. 2017YFB1201204), National Natural Science Foundation of China (grant nos. 51578552 and U1334203), and Independent Research Program of Central South University (grant no. 2018zzts650).

References

[1] M. Tanabe, H. Wakui, M. Sogabe, N. Matsumoto, and Y. Tanabe, "A combined multibody and finite element approach for dynamic interaction analysis of high-speed train and railway structure including post-derailment behavior during an earthquake," *Materials Science and Engineering*, vol. 10, no. 1, article 012144, 2010.

[2] K. Nishimura, Y. Terumichi, T. Morimura, and K. Sogabe, "Development of vehicle dynamics simulation for safety analyses of rail vehicles on excited tracks," *Journal of Computational and Nonlinear Dynamics*, vol. 4, no. 1, pp. 011001–011009, 2009.

[3] L. Ling, X. B. Xiao, L. Wu, and X. S. Jin, "Effect of spectrum characteristics of seismic wave on derailment of high-speed train," *Engineering Mechanics*, vol. 30, no. 1, pp. 384–393, 2013, in Chinese.

[4] Y. Xiang, Y.-F. Luo, and Z.-C. Zhu, "Estimating the response of steel structures subjected to vertical seismic excitation: idealized model and inelastic displacement ratio," *Engineering Structures*, vol. 148, pp. 225–238, 2017.

[5] E.-K. V. Mylona, A. G. Sextos, and G. E. Mylonakis, "Rotational seismic excitation effects on CIDH pile-supported bridge piers," *Engineering Structures*, vol. 138, pp. 181–194, 2017.

[6] X. Li, Z.-X. Li, and A. J. Crewe, "Nonlinear seismic analysis of a high-pier, long-span, continuous RC frame bridge under spatially variable ground motions," *Soil Dynamics and Earthquake Engineering*, vol. 114, pp. 298–312, 2018.

[7] S. Deshan, Z. Xiaohang, Y. Jingchao, and L. Qiao, "Bridge seismic damage identification based on seismic fragility analysis," *Journal of Vibration and Shock*, vol. 36, no. 16, pp. 195–201, 2017, in Chinese.

[8] W. Guo, J. L. Li, and H. Y. Liu, "The analysis of running safety of high-speed-train on bridge by using refined simulation considering strong earthquake," *Engineering Mechanics*, vol. 37, no. 1, pp. 259–264, 2018, in Chinese.

[9] X. T. Du, Y. L. Xu, and H. Xia, "Dynamic interaction of bridge-train system under non-uniform seismic ground motion," *Earthquake Engineering & Structural Dynamics*, vol. 41, no. 1, pp. 139–157, 2012.

[10] N. Zhang, H. Xia, and G. De Roeck, "Dynamic analysis of a train-bridge system under multi-support seismic excitations," *Journal of Mechanical Science and Technology*, vol. 24, no. 11, pp. 2181–2188, 2010.

[11] L. K. Chen, *Seismic responses of high-speed railway train-ballastless track-bridge system and train running safety during earthquake*, Ph.D. dissertation, Central South University, Changsha, China, 2012 in Chinese.

[12] N. Shaban, A. Caner, A. Yakut et al., "Vehicle effects on seismic response of a simple-span bridge during shake tests," *Earthquake Engineering & Structural Dynamics*, vol. 44, no. 6, pp. 889–905, 2015.

[13] T. S. Paraskeva, E. G. Dimitrakopoulos, and Q. Zeng, "Dynamic vehicle-bridge interaction under simultaneous vertical earthquake excitation," *Bulletin of Earthquake Engineering*, vol. 15, no. 1, pp. 71–95, 2017.

[14] M. Gao, *Earthquake Intensity Zoning Map of China: Recommendation: GB 18306-2015*, China Standard Press, Beijing, China, 2015, in Chinese.

[15] L. Xue-Yi, P.-R. Zhao, R.-S. Yang et al., *Design Theory and Methods of Ballestless Track of Passenger Dedicated Line*, Southwest Jiaotong University Press, Chengdu, China, 2010, in Chinese.

[16] P. Wang, L. Gao, L. Zhao et al., "Study on setting method of position-limitation recess of CRTSIII slab track on subgrade," *Engineering Mechanics*, vol. 31, no. 2, pp. 110–116, 2014, in Chinese.

[17] China Planning Press, *Code for Seismic Design of Railway Engineering (GB 50111-2006)*, China Planning Press, Beijing, China, 2009, in Chinese.

[18] M. Paz, *Structural Dynamics: Theory and Computation*, Chapman & Hall, New York, NY, USA, 4th edition, 1997.

[19] J. L. Humar, *Dynamics of Structures*, A. A. Balkema Publishers, Avereest, Netherlands, 2nd edition, 2002.

[20] China Railway Eryuan Engineering Group Co., Ltd., *Technical Summary of CRTSIII Slab Ballastless Track on Chengdu-Dujiangyan Railway*, China Railway Eryuan Engineering Group Co., Ltd., Chengdu, China, 2010, in Chinese.

[21] Chinese Plan Publishing House, *Dynamic Performance Criteria and Test Evaluation Standard of Railway Vehicle GB/T. 5599—1985*, Chinese Plan Publishing House, Beijing, China, 1985, in Chinese.